Plasmid-Chromosome Crosstalk in *Staphylococcus aureus*: A Horizontally Acquired Transcription Regulator Controls Polysaccharide Intercellular Adhesin-Mediated Biofilm Formation

Gabriella Marincola[1]*, Greta Jaschkowitz[1†], Ann-Katrin Kieninger[1†], Freya D.R. Wencker[1], Andrea T. Feßler[2], Stefan Schwarz[2] and Wilma Ziebuhr[1]*

[1] Institute of Molecular Infection Biology, University of Würzburg, Würzburg, Germany, [2] Centre for Infection Medicine, Institute of Microbiology and Epizootics, Free University of Berlin, Berlin, Germany

Livestock-associated methicillin-resistant *Staphylococcus aureus* (LA-MRSA) of clonal complex CC398 typically carry various antimicrobial resistance genes, many of them located on plasmids. In the bovine LA-MRSA isolate Rd11, we previously identified plasmid pAFS11 in which resistance genes are co-localized with a novel *ica*-like gene cluster, harboring genes required for polysaccharide intercellular adhesin (PIA)-mediated biofilm formation. The *ica* genes on pAFS11 were acquired in addition to a pre-existing *ica* locus on the *S. aureus* Rd11 chromosomal DNA. Both loci consist of an *icaADBC* operon and *icaR*, encoding a corresponding *icaADBC* repressor. Despite carrying two biofilm gene copies, strain Rd11 did not produce PIA and transformation of pAFS11 into another *S. aureus* strain even slightly diminished PIA-mediated biofilm formation. By focusing on the molecular background of the biofilm-negative phenotype of pAFS11-carrying *S. aureus*, we identified the pAFS11-borne *ica* locus copy as functionally fully active. However, transcription of both plasmid- and core genome-derived *icaADBC* operons were efficiently suppressed involving IcaR. Surprisingly, although being different on the amino acid sequence level, the two IcaR repressor proteins are mutually replaceable and are able to interact with the *icaA* promoter region of the other copy. We speculate that this regulatory crosstalk causes the biofilm-negative phenotype in *S. aureus* Rd11. The data shed light on an unexpected regulatory interplay between pre-existing and newly acquired DNA traits in *S. aureus.* This also raises interesting general questions regarding functional consequences of gene transfer events and their putative implications for the adaptation and evolution of bacterial pathogens.

Keywords: *Staphylococcus aureus*, biofilm regulation, PIA/*ica*, IcaR, horizontal gene transfer, plasmid-chromosome crosstalk

INTRODUCTION

Staphylococcus aureus is a common human and animal pathogen, causing a wide range of clinical manifestations (Tong et al., 2015; Ballhausen et al., 2017). Due to the capability to readily acquire many different resistance genes, *S. aureus* and other staphylococcal species are regarded as pathogens of concern for public health (Foster, 2017; Lakhundi and Zhang, 2018). Thus, methicillin-resistant *S. aureus* (MRSA) and coagulase-negative staphylococci (MR-CoNS) are among the most common causes of healthcare-associated infections (Lee et al., 2018a; Becker et al., 2020). In this respect, the ability to form biofilms on the inert surfaces of medical devices is considered as important pathomechanism that contributed to the establishment of staphylococci as notorious nosocomial pathogens (Heilmann et al., 2019; Becker et al., 2020; Schilcher and Horswill, 2020). Biofilms are understood as bacterial communities that adhere to surfaces by encasing into a self-produced extracellular polymeric matrix (Costerton et al., 1999). The staphylococcal biofilm matrix may contain exopolysaccharides (Heilmann et al., 1996) and proteins (Rohde et al., 2005) as well as extracellular (e)DNA (Qin et al., 2007) [for a recent review see reference (Schilcher and Horswill, 2020)]. The key exopolysaccharide component of staphylococcal biofilms is PIA (polysaccharide intercellular adhesin), a beta-1,6 linked N-acetyl glucosaminoglycan, whose synthesis enzymes are encoded by the *ica* (intercellular adhesin) locus [recently reviewed in (Nguyen et al., 2020)]. PIA/*ica* was originally discovered in *Staphylococcus epidermidis* and was later also detected in *S. aureus* and other staphylococcal species (Heilmann et al., 1996; Mack et al., 1996; Cramton et al., 1999). Interestingly, *ica* locus homologs also exist in phylogenetically unrelated bacteria such as *Escherichia coli* (Wang et al., 2004), suggesting an eminent role of the factor in the evolution of bacterial biofilm functions. In these organisms, PIA is also often referred to as PNAG (poly-1,6-N-acetylglucosamine). The staphylococcal *ica* locus consists of two divergently oriented transcription units, one comprising the *icaADBC* operon (encoding the enzymes required for PIA synthesis) and the other harboring *icaR* which codes for a transcription factor of the TetR family (**Figure 1A**). IcaR, for which the crystal structure was solved, binds to a region upstream of *icaA* and represents a potent repressor of *icaADBC* operon transcription (Conlon et al., 2002a; Jefferson et al., 2004; Jeng et al., 2008). Regulation of the *ica* locus is highly complex and a plethora of environmental cues are known to influence PIA production many of which either directly or indirectly influencing *icaR* transcription (Conlon et al., 2002b; Cerca et al., 2008; Fey and Olson, 2010; Cue et al., 2012; Hoang et al., 2019; Nguyen et al., 2020). Expression of *icaR* is further controlled post-transcriptionally through RNA-mediated mechanisms that influence stability and translation of the *icaR* mRNA, with direct consequences for PIA production and biofilm formation (Ruiz de los Mozos et al., 2013; Rochat et al., 2018; Bronesky et al., 2019; Lerch et al., 2019; Schoenfelder et al., 2019). While nearly all *S. aureus* genomes carry the *ica* locus,

distribution of the gene cluster among *S. epidermidis* and other CoNS species is more diverse and often associated with distinct clonal lineages (Kozitskaya et al., 2005; Conlan et al., 2012; Thomas et al., 2014; Méric et al., 2015; Méric et al., 2018; Lee et al., 2018b; Espadinha et al., 2019). The *ica* locus is usually located in the bacterial chromosomal DNA in all staphylococcal species. Previously, however, we detected an *ica* gene cluster of unknown genetic origin on plasmid pAFS11 in the bovine MRSA isolate *S. aureus* Rd11 (Feßler et al., 2017). *S. aureus* Rd11 is a livestock-associated (LA)-MRSA strain of sequence type ST398, a clonal lineage known for its potential to carry a broad range of both common and novel antibiotic resistance genes, many of which located on plasmids (Kadlec et al., 2012; Feßler et al., 2018). On pAFS11, antimicrobial and heavy metal resistance genes were found to be co-localized with a novel *ica* gene cluster. The *ica* locus on pAFS11 differed both on nucleotide and protein levels from the copy in the *S. aureus* Rd11 chromosome, and initial analyses (*i.e.* BLAST searches against the entire non-redundant sequence collections at NCBI) suggested that the plasmid-borne *ica* locus might have its origin in the CoNS species *Staphylococcus sciuri* [recently re-classified as *Mammaliicoccus sciuri* (Madhaiyan et al., 2020)] (Feßler et al., 2017). The mosaic structure of pAFS11 further suggests that the plasmid arose by a series of recombination events and was acquired by *S. aureus* Rd11 through horizontal gene transfer (HGT). As a result, *S. aureus* Rd11 carries two *ica* loci. Surprisingly, however, the strain did not produce biofilm when tested in standard tissue culture plate assays. Also, transformation of the pAFS11 plasmid into another *S. aureus* strain did not prompt biofilm formation, but even slightly reduced it (Feßler et al., 2017). In this study, we address the molecular mechanism underlying the biofilm-negative phenotype of pAFS11-bearing *S. aureus*. We identified an unexpected IcaR-mediated regulatory crosstalk between the plasmid-borne and chromosomally encoded *ica* loci, resulting in downregulation of biofilm formation. We discuss these findings in the context of co-evolution of virulence and resistance traits and raise the question of how genes newly acquired by HGT might become integrated into the regulatory network of host bacteria.

MATERIALS AND METHODS

Sequence Alignments and Data Base Searches

Alignments of the nucleotide sequences of *ica* loci as well as that of amino acid sequences of Ica proteins from different species were performed with CLUSTAL Omega multiple sequence alignments (https://www.ebi.ac.uk/Tools/msa/clustalo) (Madeira et al., 2019). Average distance between the *ica* loci and pairwise alignments were calculated with the aid of Jalview (Waterhouse et al., 2009). Strains and sequences included into the analyses comprised *S. epidermidis* RP62A (accession no. NC_002976), *S. epidermidis* O-47 (accession no.
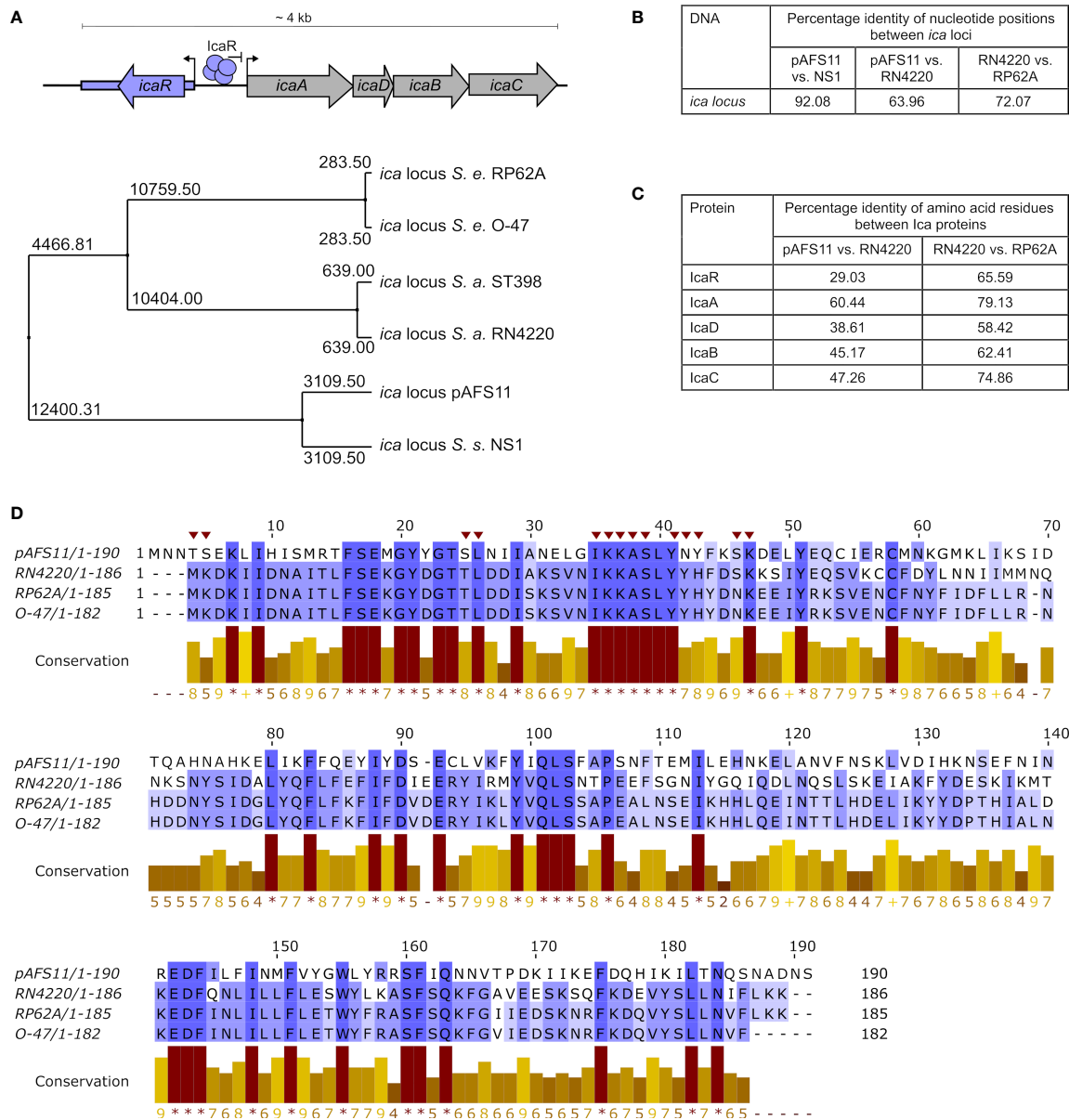
FIGURE 1 | Conservation of pAFS11 *ica* locus. **(A)** TOP: schematic view of the organization of the *ica* locus including the IcaR tetramer and its function as repressor of transcription. BOTTOM: average distances between the *ica* loci of *S. epidermidis* O-47, *S. epidermidis* RP62A, *S. aureus* RN4220, *S. aureus* lineage ST398, *S. sciuri* NS1 and plasmid pAFS11. **(B)** Pairwise Alignment shown as percentage identity of nucleotide positions between the *ica* loci of pAFS11 vs. NS1, pAFS11 vs. RN4220 and RN4220 vs. RP62A. **(C)** Pairwise Alignment shown as percentage identity of amino acid residues between the Ica proteins of RN4220 vs. pAFS11 and RN4220 vs. RP62A. **(D)** Multiple sequence alignment of IcaR protein from pAFS11, RN4220, RP62A and O-47. Conservation is visualized as a histogram and a score is given for each column: conserved residues are indicated by '*', and columns with residues, where all properties are conserved are marked with '+'. Putative *icaA* operon- interacting residues on IcaR in *S. epidermidis* are marked with a red triangle on top of the sequence (Jeng et al., 2008). All comparisons shown in **(A–D)** were calculated with the aid of Jalview (Waterhouse et al., 2009) from CLUSTAL Omega multiple sequence alignments (Madeira et al., 2019).

CP040883), *S. aureus* ST398 (accession no. AM990992.1), *S. aureus* RN4220 (accession no. AFGU01000118.1), *S. sciuri* NS1 (accession no. LDTK01000031.1) and plasmid pAFS11 (accession no. FN806789.3). Data base queries with nucleotide and protein sequences were performed using the Basic Local Alignment Search Tool available at the National Center for

Biotechnology Information (NCBI) (https://blast.ncbi.nlm.nih.gov/Blast.cgi).

Plasmid and Strain Construction

Strains, plasmids and oligonucleotides used for this work are listed in **Tables 1** and **2**, respectively.

TABLE 1 | Strains and plasmids.

	Description	Reference
Strains		
E. coli		
DC10B	*E. coli* for plasmid transformation into staphylococci	(Monk et al., 2012)
S. aureus		
RN4220	Restriction-deficient *S. aureus* strain	(Nair et al., 2011)
Rd11	LA-MRSA carrying pAFS11 plasmid	(Feßler et al., 2017)
N2	RN4220 transformed with pAFS11	(Feßler et al., 2017)
GAM20	RN4220 transformed with pGM10 (p*ica*$_{pAF}$)	This work
GAM28	RN4220 transformed with pGM11 (p*ica*$_{pAF}$_Δ*icaR*$_{pAF}$)	This work
AK18	RN4220 transformed with pAK17	This work
GAM30	RN4220 Δ*ica*	This work
GAM33	GAM30 (RN4220 Δ*ica*) transformed with pGM10 (p*ica*$_{pAF}$)	This work
GAM35	GAM30 (RN4220 Δ*ica*) transformed with pGM11 (p*ica*$_{pAF}$_Δ*icaR*)	This work
GAM42	GAM30 (RN4220 Δ*ica*) transformed with pGM12 (p*ica*$_{RN}$)	This work
GAM44	GAM30 (RN4220 Δ*ica*) transformed with pGM13 (p*ica*$_{RN}$_Δ*icaR*)	This work
GAM46	GAM30 (RN4220 Δ*ica*) transformed with pGM14 (p*ica*$_{RN}$_Δ*icaR*_*icaR*$_{pAF}$)	This work
GAM49	GAM30 (RN4220 Δ*ica*) transformed with pGM15 (p*ica*$_{pAF}$_Δ*icaR*_*icaR*$_{RN}$)	This work
GAM57	GAM30 (RN4220 Δ*ica*) transformed with pGM16 (p*ica*$_{pAF(A***)}$)	This work
GAM59	GAM30 (RN4220 Δ*ica*) transformed with pGM17 (p*ica*$_{pAF(A***)}$_Δ*icaR*)	This work
GAM61	GAM30 (RN4220 Δ*ica*) transformed with pGM18 (p*ica*$_{pAF(A***)}$_Δ*icaR*_*icaR*$_{RN}$)	This work
GAM63	GAM30 (RN4220 Δ*ica*) transformed with pGM19 (p*ica*$_{pAF(B***)}$)	This work
GAM65	GAM30 (RN4220 Δ*ica*) transformed with pGM20 (p*ica*$_{pAF(B***)}$_Δ*icaR*)	This work
GAM67	GAM30 (RN4220 Δ*ica*) transformed with pGM21 (p*ica*$_{pAF(B***)}$_Δ*icaR*_*icaR*$_{RN}$)	This work
Others		
RP62A	*S. epidermidis* biofilm positive reference strain	(Gill et al., 2005)
TM300	*S. carnosus* biofilm negative reference strain	(Que et al., 2005)
Plasmids		
pAFS11	Original plasmid isolated from Rd11	(Feßler et al., 2017)
***icaADBC* mutant construction**		
pBASE6	Suicide mutagenesis vector	(Geiger et al., 2012)
pAK17	pBASE carrying *ica*$_{RN}$ flanking region for *ica* deletion	This work
***ica* complementation**		
pRB473	Staphylococcal shuttle vector	(Brückner et al., 1993)
pGM10	pRB473 with *ica* operon from pAFS11 (*ica*$_{pAF}$)	This work
pGM11	pRB473 with *ica*$_{pAF}$_Δ*icaR*	This work
pGM12	pRB473 with *ica* operon from RN4220 (*ica*$_{RN}$)	This work
pGM13	pRB473 with *ica*$_{RN}$_Δ*icaR*	This work
pGM14	pRB473 with *ica*$_{RN}$_Δ*icaR*_*icaR*$_{pAF}$ ("crosstalk plasmid")	This work
pGM15	pRB473 with *ica*$_{pAF}$_Δ*icaR*_*icaR*$_{RN}$ ("crosstalk plasmid")	This work
pGM16	pRB473 with *ica*$_{pAF}$ with palindrome A mutated (*ica*$_{pAF(A***)}$)	This work
pGM17	pRB473 with *ica*$_{pAF(A***)}$_Δ*icaR*	This work
pGM18	pRB473 with *ica*$_{pAF(A***)}$_Δ*icaR*_*icaR*$_{RN}$	This work
pGM19	pRB473 with *ica*$_{pAF}$ with palindrome B mutated (*ica*$_{pAF(B***)}$)	This work
pGM20	pRB473 with *ica*$_{pAF(B***)}$_Δ*icaR*	This work
pGM21	pRB473 with *ica*$_{pAF(B***)}$_Δ*icaR*_*icaR*$_{RN}$	This work

*"***" symbolized mutated palindromes.*

Construction of a Markerless *icaADBC* Mutant

The markerless *ica* mutant was obtained *via* allelic replacement with inducible counter-selection using the pBASE6 shuttle vector (Bae and Schneewind, 2006; Geiger et al., 2012). pBASE6 vector was linearized using primers SLIC_pBASE_R and SLIC_pBASE_F. Total deletion was achieved by overlapping PCR using as template gDNA from RN4220 with primers Flank_A_SLIC together with Flank_A_rev and Flank_B_rev together with Flank_B_SLIC. The amplicon was introduced into the linearized pBASE6 vector using the *in vivo E. coli* cloning (iVEC) method (Nozaki and Niki, 2019). The resulting plasmid (pAK17) was transformed into the restriction-deficient strain RN4220. Mutagenesis was performed as described elsewhere (Bae and Schneewind, 2006). The deletion was verified by PCR with oligonucleotides spanning the deletion region.

Construction of Complementation Plasmids

All plasmids were created following the iVEC method (Nozaki and Niki, 2019). As iVEC turned out to be more efficient in the presence of buffer, the ligation buffer from the QuickLigation™ Kit (NEB, #M2200S) was added to the reactions. Sanger sequencing was used to verify accuracy of all plasmids. To create plasmids pGM10 and pGM12, the *ica*$_{pAF}$ and *ica*$_{RN}$ operons were amplified from pAFS11 and RN4220, respectively, and introduced in the linearized pRB473. Deletion of *icaR* coding regions from plasmids pGM10 and pGM12 (resulting in plasmids pGM11 and pGM13, respectively) was

TABLE 2 | Oligonucleotides.

Purpose	Template	Name	Sequence
qRT-PCR			
gyr	–	GM027	ACGGATAATTATGGTGCTGGGC
		GM028	TGCAAACCTCTCTCTGAAGTCG
icaA$_{RN}$	–	GM020	AACAGAGGTAAAGCCAACGC
		GM021	ATGGTGCATCTTGATCAACG
icaA$_{pAF}$	–	GM016	ATTTGATGTGTGTCGATGCAG
		GM017	TCCCTGTTACTGCTCCGATTG
icaR$_{pAF}$	–	GM018	ATGTTTGTATACGGATGGCTTT
		GM019	ATCAGCGTTTGACTGATTCG
***ica* deletion mutant**			
pAK17	RN4220	Flank_A_SLIC	GATCTGTCGACGATAACAGATACTATTGGAGATACT
		Flank_A_rev	ATTGGCATTGGTAAATCATGACATAGGCGCTT
		Flank_B_rev	ATGATTTACCAATGCCAATGGGAGTGGGACA
		Flank_B_SLIC	GCATGCAAGCTTGATAGGAACACCACATAATGGTA
	pBASE6	SLIC_pBASE_R	TATCGTCGACAGATCTGCGCG
		SLIC_pBASE_F	TCAAGCTTGCATGCCTGCAGAA
Deletion Confirmation		GM176	TTGCTAAAACAATACCAACAATA
		GM177	AAGGTAATCATGACAATATGAT
Complementation plasmids			
pGM10	pRB473	SLIC_pRB473_R	GTCGACTCTAGAGGATCCCCGG
		SLIC_pRB473_F	CTGCAGGCATGCAAGCTTGGATTCT
	pAFS11	GM154	CTTGCATGCCTGCAGACAGAAGACTCCTTTTTGTT
		SLIC_icaCSc_R	TCCTCTAGAGTCGACGAAGATAAACATTACCTATA
pGM12	pRB473	SLIC_pRB473_R	GTCGACTCTAGAGGATCCCCGG
		SLIC_pRB473_F	CTGCAGGCATGCAAGCTTGGATTCT
	RN4220	GM178	CTTGCATGCCTGCAGATCACATAGGCGCTTATCAAT
		GM179	TCCTCTAGAGTCGACTACGAAGTTTAAATGTGCAAT
pGM11	pGM10	GM156	GAGGCAAATGAAGATAATTCATAAAAACCTATAATGA
		GM155	GGTTTTTATGAATTATCTTCATTTGCCTCCTTTACTA
		GM157	AGGCAGTTATTGGTGCCCTTAAACG
		pRB473_MCS_F	CGTTTAAGGGCACCAATAACTGCCT
pGM13	pGM12	GM182	GTAGGGGGTTATAAAAATTTTTGTTACTAGTTTGTAATA
		GM183	AAACTAGTAACAAAAATTTTTATAACCCCCTACTGAAAATTA
		GM157	AGGCAGTTATTGGTGCCCTTAAACG
		pRB473_MCS_F	CGTTTAAGGGCACCAATAACTGCCT
pGM14	pAFS11	GM186	GTAGGGGGTTATAAAAAGTGAATAATACATCTGAGAAACTC
		GM187	ACAAACTAGTAACAAAAATTATGAATTATCAGCGTTTGACT
	pGM212	GM184	TTTTTATAACCCCCTACTGAAAATTAA
		GM185	TTTTTGTTACTAGTTTGTAATAATTAA
pGM15	RN4220	GM196	AGTAAAGGAGGCAAATGAATTGAAGGATAAGATTATTGATA
		GM197	TGTCATTATAGGTTTTTATTTCTTCAAAAATATATTTAGT
	pGM10	GM198	AAACCTATAATGACACGCCATA
		GM199	TTCATTTGCCTCCTTTACTACCTATGAATA
pGM16/pGM17/pGM18	pGM10/pGM11/pGM15	GM202	ATAGTATATCtaaaagtAAGAAAAAGGCAATGCGTTA
		GM201	acttttaGATATACTATTTTTACAAACTACCG
		GM157	AGGCAGTTATTGGTGCCCTTAAACG
		pRB473_MCS_F	CGTTTAAGGGCACCAATAACTGCCT
pGM19/pGM20/pGM21	pGM10/pGM11/pGM15	GM203	aagcaatGGGAGAAAATTATGAAAATTTTATTA
		GM204	TTTTCTCCCattgcttCGGTAGTTTGTAAAAATAGTA
		GM157	AGGCAGTTATTGGTGCCCTTAAACG
		pRB473_MCS_F	CGTTTAAGGGCACCAATAACTGCCT

achieved by overlapping PCRs which amplified the respective vectors in two fragments that overlapped in the *icaR* deletion and multiple cloning site regions. Of note, this approach left putative *icaR* 5' and 3' untranslated regions (UTRs) intact which might be involved in post-transcriptional regulation of *icaR*. *icaR*$_{pAF}$ was amplified from pAFS11 and introduced in the linearized pGM12, resulting in plasmid pGM14. *icaR*$_{RN}$ was amplified from RN4220 and introduced in the linearized pGM10, resulting in plasmid pGM15. The vectors containing mutated sequences which alter the palindromes (pGM16 to pGM21) were generated by PCR site-directed mutagenesis amplifying the original vectors (see **Table 2** for details) in two fragments that overlapped in the region containing the mutated palindrome and in the multiple cloning site region. In **Table 2**, the mutated palindrome sequences are shown as lower-case characters in the primer sequences.

Preparation of Total RNA and qRT-PCR

Total RNA of bacteria was isolated as described previously (Lerch et al., 2019). Briefly, RNA was precipitated with 1x

volume isopropanol (Sigma-Aldrich, #I9516) for 10 minutes at room temperature. Pelleted RNA was washed with 70 % ethanol and solved in RNase-free double-distilled water (ddH$_2$O). The transcript abundance of $icaA_{pAF}$, $icaR_{pAF}$ and $icaA_{RN}$ from three independent experiments was determined by real-time qRT-PCR. Thus, 5 µg of each RNA sample was treated with DNaseI (Thermofisher, #AM2235) for 45 min at 37°C and the reaction was stopped by phenol/chloroform/isoamylalcohol extraction (25:24:1, Carl Roth GmbH, #X985.2) with the aid of PLG heavy tubes (5 Prime, #2302830). RNA was precipitated overnight at -20°C with 4.67x volume ethanol/3M sodium acetate pH 6.5 (Thermofisher, #AM9740) (30:1 mix). Pelleted RNA was washed with 70% ethanol, dissolved in 30 µl RNase-free ddH$_2$O and diluted 1:10. To check for efficiency of DNA digestion, a PCR was set up with the same amount of RNA (1 µl of 1:10) and same primers used for qRT-PCR. One-step qRT–PCR was performed using an amplification kit with SYBR Green (Power SYBR^{TM}, Green RNA-to-CT^{TM} 1-Step Kit; Thermofisher, # 4389986) with the primers listed in **Table 2** and run on Biorad CFX according to the manufacturer's instructions. Transcript abundance was calculated using a logarithmic dilution series of one sample to generate a standard curve for each gene. Relative quantification of the genes of interest was expressed in relation to the expression of the constitutive reference gene gyrase B (*gyrB*). The means were calculated from three biological replicates run in technical duplicates. Statistical analysis was performed using one-way ANOVA by employing the GraphPad Prism software package.

Biofilm Assay

Biofilm formation was tested on 96-well, polystyrene tissue culture plates (Greiner Bio-One, # 655180) as described previously (Christensen et al., 1985), using Trypticase^{TM} Soy Broth (BD BBL^{TM}, #211768) supplemented with 4% NaCl as growth medium. *S. epidermidis* RP62A and *S. carnosus* TM300 were used as positive and negative controls, respectively. For strains carrying resistance genes, antimicrobial agents were used at the following concentrations: 25 µg ml^{-1} erythromycin (for both overnight and day culture) and 30 µg ml^{-1} (for overnight culture) or 10 µg ml^{-1} (for day culture) chloramphenicol. Bacterial overnight cultures were freshly diluted to OD$_{600}$ of 0.05 and 200 µl filled in each well (two technical replicates per strain). To distinguish between total, protein and PIA matrix-mediated biofilm production, three tissue culture plates were set up in parallel and incubated at 30°C for 18 h. Cultures were then discarded and adherent cells washed twice with 1x PBS buffer. The control plate for measuring the total biofilm was dried and heat-fixed at 65°C for 1 h. To discern between PIA- and protein-mediated biofilm, biofilms were either treated with 1 mg ml^{-1} proteinase K (Merck, #1245680500) for 4 h at 37°C or 40 mM NaIO$_4$ (Carl Roth GmbH, #2603.1) for 24 h at 4°C. Afterwards the plates were washed with 1x PBS, dried and heat-fixed. All three plates were stained with 10 mg ml^{-1} crystal violet (Merck, #115940) for 2 min, washed twice with double-distilled water before measuring the absorbance at 492 nm (ELISA plate reader, Multiskan Ascent). The means were calculated from three biological replicates. Statistical analysis was performed using

one-way ANOVA by employing the GraphPad Prism software package.

RESULTS

The Two *ica* Locus Copies in *S. aureus* Rd11 Are of Different Genetic Origin

We previously reported that database searches against the entire non-redundant nucleotide collection at NCBI (including whole-genome shotgun contigs) returned similarities of pAFS11 to an *ica*-like gene cluster present in some *S. sciuri* isolates [now *M. sciuri* (Madhaiyan et al., 2020)] (Feßler et al., 2017). Of note, the putative *ica* locus on pAFS11 was found to differ on nucleotide level from *ica* sequences present in *S. aureus* and *S. epidermidis* (Feßler et al., 2017). For further phylogenetic analysis, we therefore performed multiple sequence alignments of *icaR/icaADBC* nucleotide sequences from two *S. aureus* (*i.e.* RN4220 and ST398, to which Rd11 belongs) and two *S. epidermidis* (*i.e.* RP62A and O-47) strains as well as from the pAFS11 *ica* locus (referred to as ica_{pAF} hereafter). Finally, based on the nucleotide BLAST query results, an *ica*-like locus from the CoNS species *S. sciuri* was included into the analysis as well. Average distances were calculated from the alignment data and the tree displayed in **Figure 1A** illustrates that ica_{pAF} is most distantly related to the two *S. aureus*-derived *ica* loci. In addition, the two *ica* loci from *S. epidermidis* are highly divergent from ica_{pAF}, while they are closer related to *ica* from *S. aureus*. Interestingly, however, the ica_{pAF} nucleotide sequence is closely related to the *ica*-like locus from *S. sciuri* strain NS1 (**Figures 1A, B**). The data suggest that the two *ica* loci present in Rd11 are of different genetic origin, with ica_{pAF} most likely being derived from another species for which *S. sciuri* (*M. sciuri*) is a putative candidate. Although, as expected, interspecies conservation on the nucleotide level was found to be low (**Figure 1B**), the ica_{pAF} genes translate into amino acid sequences that are identified by the BLASTP algorithm as Ica-associated proteins with (again) some sequence differences between species. Thus, **Figure 1C** shows the percentage of identical amino acid positions upon pairwise alignments of Ica proteins from ica_{pAF}, *S. aureus* RN4220 and *S. epidermidis* RP62A. While comparisons between RN4220 and RP62A revealed high conservation of *S. aureus* and *S. epidermidis* Ica proteins, identical amino acid positions were much lower between ica_{pAF} and *S. aureus*-derived Ica proteins. In this respect, IcaR was the protein with the lowest conservation (29%), indicating that the two IcaR repressor proteins harbored by *S. aureus* Rd11 differ significantly on the protein sequence level (**Figure 1C**). Despite this apparent divergence, IcaR$_{pAF}$ exhibits a number of amino acid residues (marked by asterisks in the conservation histogram in **Figure 1D**) that are highly conserved in IcaR proteins of *S. aureus* and *S. epidermidis* as well (**Figure 1D**). These include the putative *icaA* operator-interacting residues shown for IcaR *S. epidermidis* (Jeng et al., 2008) (marked with red triangles on top of the sequence in **Figure 1D**).

Plasmid pAFS11 Has a Negative Effect on *S. aureus* PIA-Mediated Biofilm Formation

As mentioned above, we previously reported that *S. aureus* Rd11 carrying pAFS11 does not produce biofilm, nor does *S. aureus* RN4220 into which the plasmid was transformed, suggesting that ica_{pAF} on the plasmid might be inactive (Feßler et al., 2017). To challenge this hypothesis, we cloned the entire ica_{pAF} from pAFS11 onto the shuttle vector pRB473 (resulting in plasmid $pica_{pAF}$) to enable ready genetic manipulation of the locus. As a first step, we deleted the $icaR_{pAF}$ coding region from the vector, yielding plasmid $pica_{pAF\_\Delta icaR}$. Both plasmids (with or without $icaR_{pAF}$) were transformed into *S. aureus* RN4220 as recipient strain and biofilm assays were performed with the constructs and corresponding wild types (**Figure 2**). The biofilm assays allow to detect total biofilm formation as well as to differentiate between PIA and protein matrix-mediated biofilm production (see material and methods for details). We display here (and in the following figures) solely the data for PIA-mediated biofilm formation (**Figures 2–5**). The entire data sets on total, protein and PIA biofilm formation can be found in **Supplementary Figure S1**. The assays confirmed the PIA biofilm-negative phenotype of *S. aureus* Rd11 and revealed that the *S. aureus* RN4220 wild type is a weak, but detectable PIA biofilm producer. Upon acquisition of pAFS11, PIA biofilm formation of RN4220 did not increase, but on the contrary was even slightly reduced, although this reduction was statistically not significant (+pAFS11, **Figure 2**). The same phenomenon occurred when *S. aureus* RN4220 was transformed with plasmid $pica_{pAF}$, carrying the entire ica_{pAF} locus from pAFS11 (+$pica_{pAF}$,
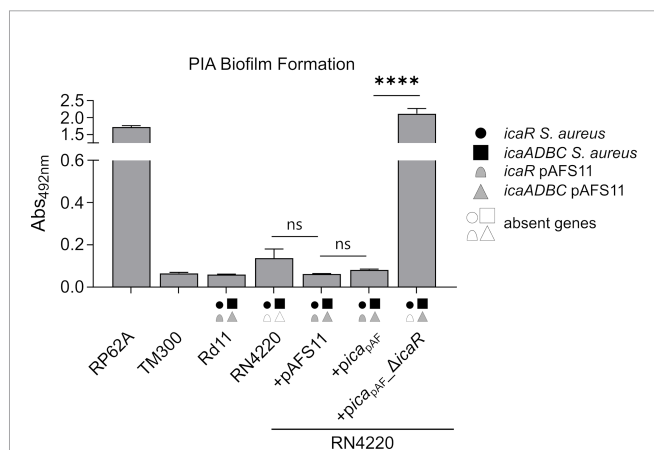

FIGURE 2 | Effect of pAFS11 on PIA biofilm formation. Analysis of PIA biofilm production by static 96-well microtiter plate biofilm assays of Rd11, RN4220 and RN4220 transformed with plasmid pAFS11 or with a plasmid carrying the whole *ica* operon from pAFS11 (+$pica_{pAF}$) or with *icaR* deletion (+$pica_{pAF\_\Delta icaR}$). RP62A served as positive control, TM300 as negative control. The means were calculated from three biological replicates run in duplicates. The *ica* genes distinctive for each strain are depicted as symbols, with filled symbols indicating presence and empty symbols indicating absence of a given gene (as indicated in the legend). The entire data sets on total, protein and PIA biofilm formation can be found in **Supplementary Figure S1**. Statistical analysis was performed using one-way ANOVA by employing the GraphPad Prism software package. ns: $P = 0.1234$; ****$P < 0.0001$.
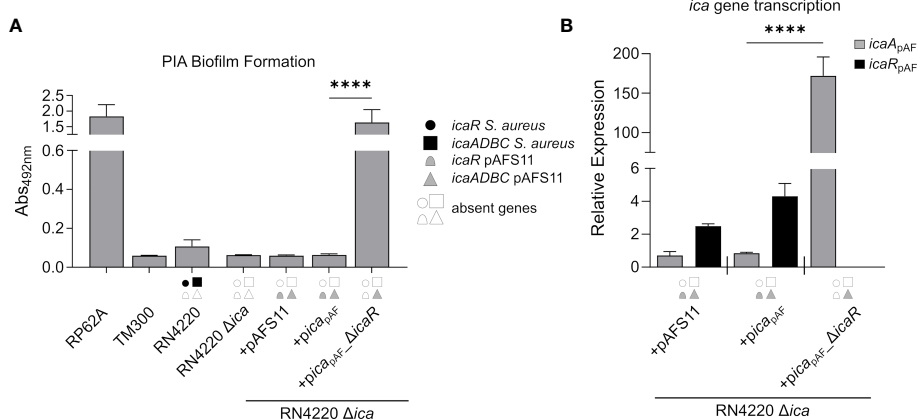
Figure 2). In contrast, however, PIA biofilm formation of RN4220 massively increased when the $icaR_{pAF}$ gene was deleted from the ica_{pAF} copy on the vector (+$pica_{pAF\_\Delta icaR}$, **Figure 2**). In the *S. aureus* RN4220 +$pica_{pAF\_\Delta icaR}$ strain, PIA biofilm levels even exceeded that of the *S. epidermidis* RP62A positive control and were much higher than in the RN4220 wild type, suggesting that the ica_{pAF} copy on the vector contributes to PIA production, but only when the $IcaR_{pAF}$ repressor is absent. We conclude from this that pAFS11 may exert its negative effect on *S. aureus* PIA biofilm formation most likely *via* $IcaR_{pAF}$ which also seems to negatively influence the *ica* locus on the RN4220 chromosome (hereinafter referred to as ica_{RN}).

The *ica* Locus on pAFS11 Is Inactive Due to Efficient IcaR Repression

The data obtained so far strongly suggest that the ica_{pAF} locus is functional and capable to enable PIA synthesis. However, by our initial experimental set-up (*i.e.* by employing the *S. aureus* RN4220 wild type with an intact chromosomal ica_{RN} locus) it was difficult to distinguish between ica_{pAF}- and ica_{RN}-derived PIA production. Therefore, we constructed a markerless ica_{RN} deletion mutant in RN4220 *via* allelic replacement, and transformed the resulting RN4220 Δica strain with plasmids pAFS11, $pica_{pAF}$ and $pica_{pAF\_\Delta icaR}$. Biofilm assays with the constructs confirmed loss of PIA production in the RN4220 Δica deletion mutant (**Figure 3A**). Providing the mutant with an entire ica_{pAF} locus either on plasmid pAFS11 or $pica_{pAF}$ did not result in biofilm formation (**Figure 3A**). However, biofilm formation was triggered and highly significantly increased, when the $icaR_{pAF}$ repressor-encoding gene was deleted from the ica_{pAF} locus (+$pica_{pAF\_\Delta icaR}$, **Figure 3A**), indicating that the $icaADBC_{pAF}$ genes of ica_{pAF} are indeed able to mediate PIA biofilm formation, once $IcaR_{pAF}$-dependent repression is alleviated. To further corroborate this assumption, we monitored transcription of $icaA_{pAF}$ and $icaR_{pAF}$ by qRT-PCR in the various constructs. In strain RN4220 Δica, transformed with either pAFS11 or $pica_{pAF}$, weak $icaA_{pAF}$ transcription was detectable (**Figure 3B**). Upon deletion of $icaR_{pAF}$ from the plasmid (+$pica_{pAF\_\Delta icaR}$, **Figure 3B**), $icaR_{pAF}$ transcription was no longer detectable (as expected) and $icaA_{pAF}$ transcription levels massively increased (*i.e.* 200-fold) compared to the intact ica_{pAF} copy (+$pica_{pAF}$, **Figure 3B**). These findings are in agreement with the biofilm test results. From the combined data we conclude that (i) the ica_{pAF} locus on pAFS11 is functionally fully intact and (ii) $icaADBC_{pAF}$ operon transcription is efficiently repressed by its cognate $IcaR_{pAF}$ repressor.

IcaR From pAFS11 Represses the *ica* Locus in the *S. aureus* Chromosomal DNA and *vice versa*

Our initial experiments with wild type *S. aureus* RN4220 indicated that $IcaR_{pAF}$ may also inhibit $icaADBC_{RN}$ expression on the RN4220 chromosome (**Figure 2**). To substantiate this hypothesis, we constructed another set of plasmids carrying (i)

FIGURE 3 | The *ica* genes of pAFS11 lead to biofilm formation. **(A)** Analysis of PIA biofilm production by static 96-well microtiter plate biofilm assays of strain RN4220 wild type and Δ*ica* alone or complemented with plasmid pAFS11 or with a plasmid carrying the whole *ica* operon from pAFS11 (+p*ica*$_{pAF}$) or with *icaR* deletion (+p*ica*$_{pAF}$_Δ*icaR*). RP62A served as positive control, TM300 as negative control. The entire data sets on total, protein and PIA biofilm formation can be found in **Supplementary Figure S1**. **(B)** Quantification of *icaA*$_{pAF}$ and *icaR*$_{pAF}$ transcripts by qRT-PCR of strains from **(A)**. The graph displays relative mRNA amounts using *gyrB* expression as reference. **(A, B)** The *ica* genes distinctive for each strain are depicted as symbols, with filled symbols indicating presence and empty symbols indicating absence of a given gene (as indicated in the legend). The means were calculated from three biological replicates run in duplicates. Statistical analysis was performed using one-way ANOVA by employing the GraphPad Prism software package. ns: $P = 0.1234$; ****$P < 0.0001$.

the *ica* locus from RN4220 (p*ica*$_{RN}$), (ii) the *ica* locus from RN4220 lacking *icaR*$_{RN}$ (p*ica*$_{RN}$_Δ*icaR*$_{RN}$) and (iii) the *ica* locus from RN4220 where we exchanged *icaR*$_{RN}$ from RN4220 with *icaR*$_{pAF}$ from pAFS11 (p*ica*$_{RN}$_Δ*icaR*$_{RN}$_*icaR*$_{pAF}$). All plasmids were transformed into the RN4220 Δ*ica* mutant background and the resulting strains were analyzed for their ability to form PIA biofilm (**Figure 4A**). Complementation of RN4220 Δ*ica* with its own *ica*$_{RN}$ locus restored PIA-mediated biofilm formation, and upon *icaR*$_{RN}$ repressor gene deletion, PIA biofilm production significantly increased, demonstrating functionality of the vector-borne *ica*$_{RN}$ locus, including *icaR*$_{RN}$-mediated regulation (**Figure 4A**). Accordingly, qRT-PCR analysis confirmed that IcaR$_{RN}$ efficiently represses transcription of its cognate *icaADBC*$_{RN}$ operon (**Figure 4B**). We then asked the question whether or not expression of the chromosomal *icaADBC*$_{RN}$ operon can undergo control by the foreign IcaR$_{pAF}$ repressor from pAFS11. Thus, we performed biofilm tests and quantitative transcription analyses with vector p*ica*$_{RN}$_Δ*icaR*_*icaR*$_{pAF}$, in which *icaADBC*$_{RN}$ was combined with the *icaR*$_{pAF}$ gene from pAFS11. As shown in **Figure 4**, presence of *icaR*$_{pAF}$ significantly diminished PIA production and transcription of the *icaADBC*$_{RN}$ operon, suggesting the capability of IcaR$_{pAF}$ to control the *icaADBC*$_{RN}$ copy from RN4220 (**Figure 4**). *Vice versa*, we next investigated, if IcaR$_{RN}$ from RN4220 can influence *icaADBC*$_{pAF}$ from pAFS11. For this purpose, we additionally constructed vector p*ica*$_{pAF}$_Δ*icaR*$_{pAF}$_*icaR*$_{RN}$ which was transformed into the RN4220 Δ*ica* mutant background. Biofilm testing revealed a highly significant reduction of PIA production when *icaADBC*$_{pAF}$ was combined with *icaR*$_{RN}$, suggesting that IcaR from *S. aureus* RN4220 is indeed able to repress the *icaADBC*$_{pAF}$ genes from pAFS11 (**Figure 4C**).

A Palindrome Sequence in the *icaA*$_{pAF}$ Upstream Region Is Required for IcaR-Mediated Biofilm Repression

The data obtained so far demonstrate that the pAFS11- and RN4220-derived IcaR repressors, which differ on amino acid level (**Figure 1D**), are able to control the *icaADBC* operon of the respective other *ica* locus copy. To understand the molecular prerequisites for the IcaR interactions with their DNA targets, we focused on the nucleotide sequence constraints known to be involved in IcaR binding. IcaR was previously shown to bind as a dimer to a specific palindrome sequence (ACCTANCTNNC/ GNNAGNTAGGT) present in the *icaA* operator of *S. epidermidis* (Jeng et al., 2008). This palindrome is 22 nucleotides long and contains six mismatches (22,6) (**Figure 5A**, top). Of note, the sequence is highly conserved and is also present in the *S. aureus icaA* promoter region (**Figure 5A**, top). Surprisingly, although IcaR from *S. aureus* is clearly able to control PIA production from pAFS11, the *S. aureus*-like palindrome sequence stretch lacks in *ica*$_{pAF}$ (**Figure 5A**, bottom). Instead, the *icaA*$_{pAF}$ upstream region displays two other palindromes which differ at the nucleotide level from that of the known *S. aureus/S. epidermidis* recognition site. Thus, palindrome A (TNAAAATNNTA/TANNATTTTNA) is 22 nucleotides long and harbors six mismatches (22,6), while palindrome B (CNAACNANC/GNTNGTTNG) consists of 18 nucleotides with six mismatches (18,6) (**Figure 5A**, bottom). To investigate the putative involvement of these palindromes in IcaR function, we mutated either palindrome A or B in (i) a plasmid carrying the whole *ica*$_{pAF}$, (ii) in an *ica*$_{pAF}$ plasmid with an *icaR*$_{pAF}$ deletion as well as (iii) in an *icaR*$_{pAF}$ deletion vector complemented with *icaR*$_{RN}$. The plasmids were again transformed into the RN4220 Δ*ica* mutant background and analyzed for PIA-mediated biofilm formation. **Figure 5B** demonstrates
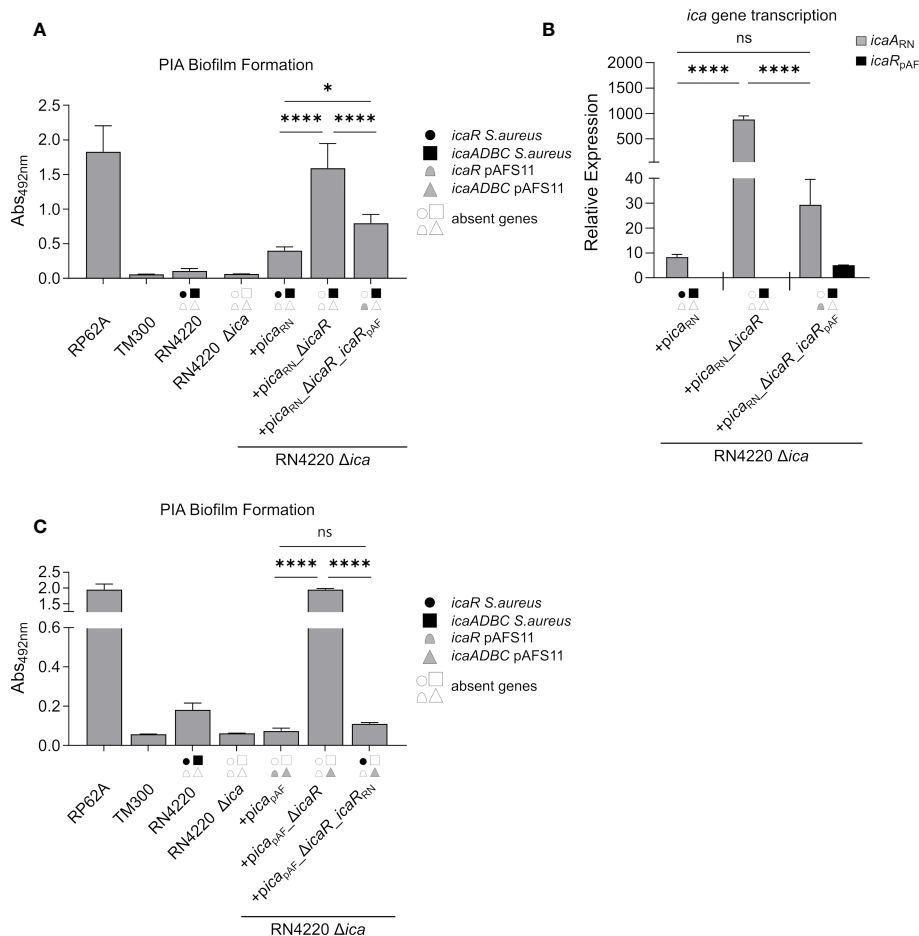
FIGURE 4 | IcaR$_{pAF}$ controls expression of *ica* genes from RN4220 and *vice versa*. **(A)** Analysis of PIA biofilm production by static 96-well microtiter plate biofilm assays of strain RN4220 wild type and Δ*ica* alone or complemented with a plasmid carrying the *ica* operon of RN4220 (+p*ica*$_{RN}$) or with *icaR* deletion (+p*ica*$_{RN}$_Δ*icaR*) or with *icaR*$_{pAF}$ instead of *icaR*$_{RN}$ (+p*ica*$_{RN}$_Δ*icaR*_*icaR*$_{pAF}$). The entire data sets on total, protein and PIA biofilm formation can be found in **Supplementary Figure S1**. **(B)** Quantification of *icaA*$_{RN}$ and *icaR*$_{pAF}$ transcripts by qRT-PCR of complemented strains from **(A)**. The graph displays relative mRNA amounts using *gyrB* expression as reference. **(C)** Analysis of PIA biofilm production by static 96-well microtiter plate biofilm assays of RN4220 wild type and Δ*ica* alone or complemented with the *ica* operon of plasmid pAFS11 on a working plasmid (+p*ica*$_{pAF}$) or the *ica* operon of plasmid pAFS11 with *icaR* deletion (+p*ica*$_{pAF}$_Δ*icaR*) or with *icaR*$_{RN}$ instead of *icaR*$_{pAF}$ (+p*ica*$_{pAF}$_Δ*icaR*_*icaR*$_{RN}$). **(A, C)** RP62A served as positive control, TM300 as negative control. **(A–C)** The *ica* genes distinctive for each strain are depicted as symbols, with filled symbols indicating presence and empty symbols indicating absence of a given gene (as indicated in the legend). The means were calculated from three biological replicates run in duplicates. Statistical analysis was performed using one-way ANOVA by employing the GraphPad Prism software package. ns: *P* = 0.1234; **P* = 0.0332; *****P* < 0.0001.

that an altered palindrome A sequence did not influence *icaR*-mediated biofilm control. Thus, upon palindrome A mutation, PIA-mediated biofilm production remained repressed in p*ica*$_{pAF(A***)}$, indicating that IcaR$_{pAF}$ does not require this nucleotide sequence stretch for action. As expected, PIA production was derepressed when *icaR*$_{pAF}$ was lacking in the palindrome A mutant (+p*ica*$_{pAF(A***)}$_Δ*icaR*, **Figure 5B**). Most importantly, however, *icaR*$_{RN}$ was still able to completely downregulate PIA-mediated biofilm production in this construct, confirming that palindrome A is not an interaction site for IcaR, neither for IcaR proteins derived from pAFS11 nor from RN4220 (**Figure 5B**). In contrast, mutation of palindrome B had a profound impact on biofilm regulation by IcaR. Firstly, PIA production was found to be deregulated and increased in

an *ica*$_{pAF}$ construct carrying an altered palindrome B nucleotide sequence (+p*ica*$_{pAF(B***)}$), suggesting that control by the cognate IcaR$_{pAF}$ is significantly impaired when integrity of this sequence stretch is disturbed (**Figure 5B**). Moreover, PIA-mediated biofilm production further increased in a palindrome B mutant in which *icaR*$_{pAF}$ was deleted (+p*ica*$_{pAF(B***)}$_Δ*icaR*, **Figure 5B**), which speaks in favor of residual IcaR$_{pAF}$ repressor activity in the palindrome B mutant. Finally, when providing the mutant with IcaR$_{RN}$ from RN4220, biofilm repression was partially, but not fully restored which (again) is in good agreement with residual IcaR repression in the palindrome B mutant. Together, the combined data strongly suggest that IcaR from both pAFS11 and RN4220 require an intact palindrome B (but not palindrome A) for unfolding their repressor activity on the *ica*$_{pAF}$ locus.
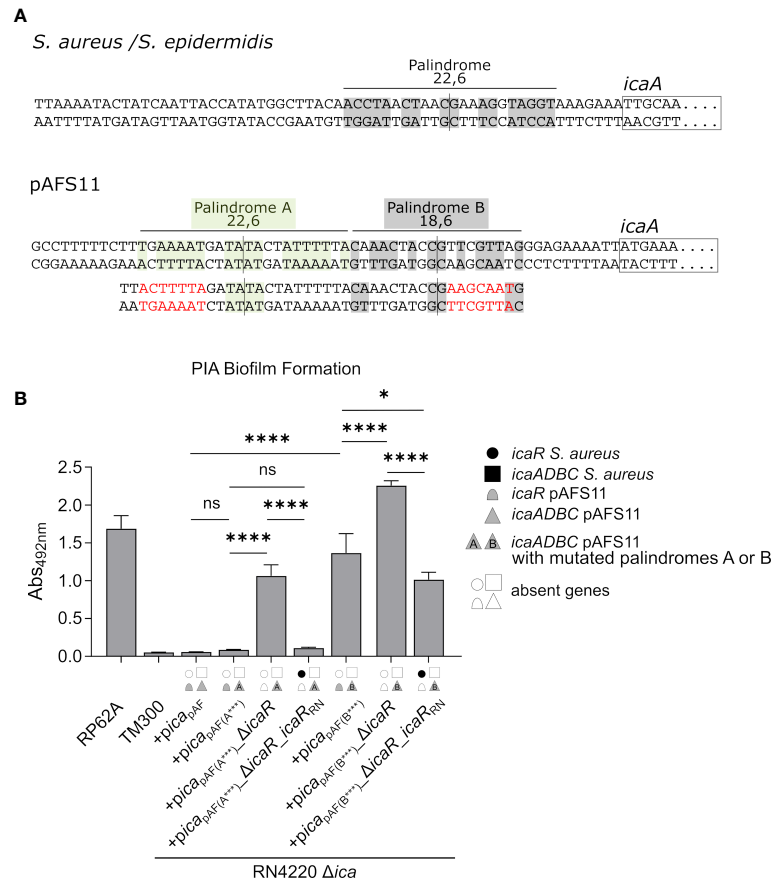
FIGURE 5 | IcaR proteins from *S. aureus* and from pAFS11 require a palindrome on the *icaA*pAF operator for action. **(A)** TOP: Known palindrome sequence on *S. aureus/S. epidermidis* is shown at the top of the panel (Jeng et al., 2008). 22,6 stands for a palindrome which is 22 nt long and carries six mismatches. BOTTOM: Putative palindromes A and B on *icaA*pAF operator are shown and their characteristics are reported. The nucleotide mutations introduced are shown in red below the wild type sequence alongside with the resulting palindrome perturbations. **(B)** Analysis of PIA biofilm production by static 96-well microtiter plate biofilm assays of strain RN4220 Δ*ica* complemented with the *ica* operon from pAFS11 wild type (+p*ica*pAF) or with deletion of *icaR*pAF (+p*ica*pAF_Δ*icaR*) or with *icaR*RN instead of *icaR*pAF (+p*ica*pAF_Δ*icaR_icaR*RN), carrying a mutated palindrome A (*ica*pAF(A***)) or B (*ica*pAF(B***)). The *ica* genes distinctive for each strains are depicted as symbols, with filled symbols indicating presence and empty symbols indicating absence of a given gene (as indicated in the legend). The entire data sets on total, protein and PIA biofilm formation can be found in **Supplementary Figure S1**. The means were calculated from three biological replicates run in duplicates. Statistical analysis was performed using one-way ANOVA by employing the GraphPad Prism software package. ns: $P = 0.1234$; *$P = 0.0332$; ****$P < 0.0001$.

DISCUSSION

Acquisition of mobile genetic elements (MGEs) is often beneficial for bacteria by providing novel metabolic and resistance traits. However, MGE carriage may also come at considerable cost for the recipient bacterial cell (Slater et al., 2008; San Millan and MacLean, 2017). Thus, resources will be required to replicate and maintain MGEs (*e.g.* plasmids) on which beneficial genes are located and their (inappropriate) expression may impose a metabolic burden, resulting in reduced fitness and competitiveness of MGE-bearing bacterial cells (Baltrus, 2013). Accordingly, bacteria have evolved sophisticated mechanisms to control both MGE uptake and maintenance as well as expression of horizontally acquired genes (Brantl, 2014; Kwong et al., 2017; Firth et al., 2018). In case of plasmid-mediated HGT, this often involves a regulatory crosstalk between chromosomal factors and the newly acquired plasmid (Huang et al., 1990; Charles and Nester, 1993; Baños et al., 2009). Interestingly, these control networks are not unidirectional and there is growing evidence to suggest that plasmids are able to influence chromosomal gene expression as well in a wide range of bacterial species [recently reviewed in (Vial and Hommais, 2020)]. In the study presented here, we extend these examples by the Gram-positive pathogen *S. aureus* and reveal that horizontally acquired and core genome genes have the capacity to mutually influence each other in this organism. Thus, we demonstrate that a transcription factor (*i.e.* IcaR), located on a large multi-resistance plasmid, is able to target a pathogenicity factor (*i.e. icaADBC*-mediated PIA biofilm formation) from the *S. aureus* core genome. *Vice versa*, the IcaR homolog from the *S. aureus* core genome was found to be able to silence transcription of plasmid-borne *icaADBC* genes, creating a

bi-directional regulatory crosstalk between plasmid- and chromosomally encoded factors that eventually hindered metabolically costly PIA-mediated biofilm formation.

PIA consists of N-acetyl-glucosamines (GlcNac) molecules, and ample sugar and energy supplies are fuelled into GlcNac synthesis to provide the building blocks of the exopolysaccharide. Accordingly, *ica* gene expression is intimately linked to central carbon flux control and energy balance (Vuong et al., 2005; Seidl et al., 2008; Zhu et al., 2009; Sadykov et al., 2011; Lindgren et al., 2014) which also involves the action of non-coding RNAs to appropriately adjust metabolic patterns (Rochat et al., 2018; Bronesky et al., 2019; Marincola et al., 2019; Schoenfelder et al., 2019). Presence of two fully functional *ica* gene clusters in strain *S. aureus* Rd11 is likely to represent a major metabolic challenge and the observed downregulation of PIA production in this strain makes sense to prevent metabolic overload. Paradoxically, it is just the additionally acquired ica_{pAF} locus copy on plasmid pAFS11 that mediates a biofilm-negative phenotype. Indeed, acquisition of pAFS11 or the ica_{pAF} locus alone abolished PIA biofilm formation in *S. aureus* (**Figure 2**). This effect is accomplished through the $IcaR_{pAF}$ repressor which can also target the chromosomal *ica* locus copy (**Figure 4**). Moreover, the tight self-control of the ica_{pAF} copy on pAFS11 by its cognate $IcaR_{pAF}$ repressor further contributes to a biofilm-negative phenotype (**Figures 2**, **3**). Remarkably, $icaADBC_{pAF}$ expression can be additionally repressed by Ica_{RN} from the core genome (**Figure 4C**). Thus, although being different from the canonical IcaR recognition site known from *S. epidermidis* and *S. aureus* (Jeng et al., 2008), Ica_{RN} interacts with a palindrome sequence present in the upstream region of $icaADBC_{pAF}$ (palindrome B in **Figure 5A**), revealing a certain flexibility of IcaR-like proteins in DNA target selection (**Figure 5**).

Phylogenetic analyses revealed that the two *ica* loci in Rd11 differ both on nucleotide and protein sequence levels and are only distantly related to each other (**Figure 1**). Thus, the horizontally acquired ica_{pAF} copy on pAFS11 is likely to originate from an unknown bacterium for which the soil and animal dwelling species *S. sciuri* [recently re-classified as *M. sciuri* (Madhaiyan et al., 2020)] might represent a putative candidate (Feßler et al., 2017). But clearly more detailed investigations will be required to substantiate this hypothesis. Interestingly, inhibition of core genome-encoded exopolysaccharide production by plasmids seems to be a common theme in the bacterial world. Thus, in nitrogen-fixing *Rhizobium tropici*, exopolysaccharide production was found to be downregulated by the NrcR transcription factor, encoded on an acquired plasmid (Del Cerro et al., 2016), and in the nosocomial pathogen *Acinetobacter baumanii*, PNAG (PIA) production was described to be diminished upon acquisition of a multi-resistance plasmid (Venanzio et al., 2019). In the latter case, this large conjugative multiresistance plasmid facilitates its own transmission by downregulating chromosomally encoded type-6-secretion systems (T6SS) that usually hamper HGT (Venanzio et al., 2019). Together with the effect on PNAG production, the *A. baumanii* plasmids represent interesting examples for a plasmid-chromosome regulatory crosstalk that influences simultaneously both virulence and resistance traits.

LA-MRSA lineages of the clonal complex CC398 (to which strain Rd11 belongs to) can thrive in very different habitats (*e.g.* animals, humans, environment etc.) where they are exposed to numerous stress conditions. It is tempting to speculate that PIA biofilm formation, which is an important factor in *S. aureus* pathogenesis and survival (Fluckiger et al., 2005; Kropec et al., 2005), might become a selection advantage at some stage. In this respect, it is an interesting question by which mechanism(s) biofilm formation could be restored in the Rd11 isolate. Plasmid pAFS11 displays a striking mosaic structure and has most likely arisen by recombination of genes from various origins. Assuming that ica_{pAF} locus integration into pAFS11 and acquisition of the plasmid by *S. aureus* is an evolutionarily recent event, it is conceivable that control of pAFS11-encoded gene expression is not fully integrated into the regulatory network of the *S. aureus* Rd11 recipient (yet). One obvious possibility to (re)gain a biofilm positive phenotype would be (spontaneous) mutation and inactivation of $icaR_{pAF}$ on pAFS11. At first sight, this idea seems to be contradictory to our experimental findings showing that $IcaR_{RN}$ has the potential to take over and replace the lacking $IcaR_{pAF}$ activity. This mutual IcaR replacement seems to work particularly well, when both factors (*icaR* and *icaADBC*) are on the same replicon and are probably in an appropriate stoichiometric repressor/DNA equilibrium (**Figure 4C**). In agreement with this assumption, the $IcaR_{RN}$ repressor effect was found to be less efficient when a single $icaR_{RN}$ copy resides on the chromosome and $icaADBC_{pAF}$ is located on a (multi-copy) plasmid (**Figure 2**). Here, $icaR_{pAF}$ deletion on the vector enabled PIA production, and it is reasonable to suggest that the insufficient repressor activity of Ica_{RN} in this experimental set-up might be associated with the copy number of the ica_{pAF}-bearing vector which increased the number of DNA targets for the $IcaR_{RN}$ repressor. At the present stage of experimental work this is mere speculation. However, recent research demonstrates that available IcaR protein amounts are critical for the appropriate control of *icaADBC* transcription, and multiple *cis*- and *trans*-acting factors have been identified that target *icaR* mRNA molecules to fine-tune their translation (Ruiz de los Mozos et al., 2013; Rochat et al., 2018; Bronesky et al., 2019; Lerch et al., 2019; Schoenfelder et al., 2019). Plasmid copy number effects may have the potential to interfere with this delicate repressor/DNA target balance. In this respect, the data obtained with ica_{pAF}-bearing plasmids in the ica_{RN} locus proficient *S. aureus* RN4220 background may reflect very well the natural situation in pAFS11 carrying isolates (**Figure 2**). Thus, from an evolutionary point of view, mutational inactivation of $icaR_{pAF}$ on the pAFS11 plasmid would make sense to readily enable PIA production. The same effect could be achieved by acquiring mutations in the ica_{pAF} palindrome B sequence, which represents the target site of both the $IcaR_{pAF}$ and $IcaR_{RN}$ proteins. Indeed, at least for *S. aureus* core genome *ica* loci, mutations in *icaA* upstream regions were previously described. The mutations had direct consequences for PIA production and occurred both *in vitro* and *in vivo*, indicating that the *icaA* promoter region undergoes selection and is a

suitable target to modulate PIA production (Jefferson et al., 2003; Schwartbeck et al., 2016). It will be interesting to explore if the ica_{pAF} locus on pAFS11 might become subject to mutational variation. Long-term *in vitro* passage experiments together with surveillance of the evolution of pAFS11-like plasmids in field studies will be suitable approaches to give answers to how control of plasmid-borne *ica* locus expression will be integrated into the regulatory network of *S. aureus*.

DATA AVAILABILITY STATEMENT

The original contributions presented in the study are included in the article/**Supplementary Material**. Further inquiries can be directed to the corresponding authors.

AUTHOR CONTRIBUTIONS

FUNDING

ACKNOWLEDGMENTS

SUPPLEMENTARY MATERIAL

The Supplementary Material for this article can be found online at: https://www.frontiersin.org/articles/10.3389/fcimb.2021.660702/full#supplementary-material

REFERENCES

Bae, T., and Schneewind, O. (2006). Allelic replacement in *Staphylococcus aureus* with inducible counter-selection. *Plasmid* 55, 58–63. doi: 10.1016/j.plasmid.2005.05.005

Ballhausen, B., Kriegeskorte, A., van Alen, S., Jung, P., Köck, R., Peters, G., et al. (2017). The pathogenicity and host adaptation of livestock-associated MRSA CC398. *Vet. Microbiol.* 200, 39–45. doi: 10.1016/j.vetmic.2016.05.006

Baltrus, D. A. (2013). Exploring the costs of horizontal gene transfer. *Trends Ecol. Evol.* 28, 489–495. doi: 10.1016/j.tree.2013.04.002

Baños, R. C., Vivero, A., Aznar, S., García, J., Pons, M., Madrid, C., et al. (2009). Differential regulation of horizontally acquired and core genome genes by the bacterial modulator H-NS. *PLoS Genet.* 5, e1000513. doi: 10.1371/journal.pgen.1000513

Becker, K., Both, A., Weißelberg, S., Heilmann, C., and Rohde, H. (2020). Emergence of coagulase-negative staphylococci. *Expert Rev. Anti Infect. Ther.* 18, 349–366. doi: 10.1080/14787210.2020.1730813

Brantl, S. (2014). Plasmid Replication Control by Antisense RNAs. *Microbiol. Spectr.* 2, PLAS-0001-2013. doi: 10.1128/microbiolspec.PLAS-0001-2013

Bronesky, D., Desgranges, E., Corvaglia, A., François, P., Caballero, C. J., Prado, L., et al. (2019). A multifaceted small RNA modulates gene expression upon glucose limitation in *Staphylococcus aureus*. *EMBO J.* 38, e99363. doi: 10.15252/embj.201899363

Brückner, R., Wagner, E., and Götz, F. (1993). Characterization of a sucrase gene from *Staphylococcus xylosus*. *J. Bacteriol.* 175, 851–857. doi: 10.1128/jb.175.3.851-857.1993

Cerca, N., Brooks, J. L., and Jefferson, K. K. (2008). Regulation of the intercellular adhesin locus regulator (*icaR*) by SarA, sigmaB, and IcaR in *Staphylococcus aureus*. *J. Bacteriol.* 190, 6530–6533. doi: 10.1128/JB.00482-08

Charles, T. C., and Nester, E. W. (1993). A chromosomally encoded two-component sensory transduction system is required for virulence of *Agrobacterium tumefaciens*. *J. Bacteriol.* 175, 6614–6625. doi: 10.1128/jb.175.20.6614-6625.1993

Christensen, G. D., Simpson, W. A., Younger, J. J., Baddour, L. M., Barrett, F. F., Melton, D. M., et al. (1985). Adherence of coagulase-negative staphylococci to plastic tissue culture plates: a quantitative model for the adherence of staphylococci to medical devices. *J. Clin. Microbiol.* 22, 996–1006. doi: 10.1128/JCM.22.6.996-1006.1985

Conlan, S., Mijares, L. A.NISC Comparative Sequencing Program, B, , Becker, J., Blakesley, R. W., Bouffard, G. G., et al. (2012). *Staphylococcus epidermidis* pan-genome sequence analysis reveals diversity of skin commensal and hospital infection-associated isolates. *Genome Biol.* 13, R64. doi: 10.1186/gb-2012-13-7-r64

Conlon, K. M., Humphreys, H., and O'Gara, J. P. (2002a). *icaR* encodes a transcriptional repressor involved in environmental regulation of *ica* operon expression and biofilm formation in *Staphylococcus epidermidis*. *J. Bacteriol.* 184, 4400–4408. doi: 10.1128/jb.184.16.4400-4408.2002

Conlon, K. M., Humphreys, H., and O'Gara, J. P. (2002b). Regulation of *icaR* gene expression in *Staphylococcus epidermidis*. *FEMS Microbiol. Lett.* 216, 171–177. doi: 10.1111/j.1574-6968.2002.tb11432.x

Costerton, J. W., Stewart, P. S., and Greenberg, E. P. (1999). Bacterial biofilms: a common cause of persistent infections. *Science* 284, 1318–1322. doi: 10.1126/science.284.5418.1318

Cramton, S. E., Gerke, C., Schnell, N. F., Nichols, W. W., and Götz, F. (1999). The intercellular adhesion (*ica*) locus is present in *Staphylococcus aureus* and is required for biofilm formation. *Infect. Immun.* 67, 5427–5433. doi: 10.1128/IAI.67.10.5427-5433.1999

Cue, D., Lei, M. G., and Lee, C. Y. (2012). Genetic regulation of the intercellular adhesion locus in staphylococci. *Front. Cell. Infect. Microbiol.* 2:38. doi: 10.3389/fcimb.2012.00038

Del Cerro, P., Rolla-Santos, A. A. P., Valderrama-Fernández, R., Gil-Serrano, A., Bellogín, R. A., Gomes, D. F., et al. (2016). NrcR, a New Transcriptional Regulator of *Rhizobium tropici* CIAT 899 Involved in the Legume Root-Nodule Symbiosis. *PLoS One* 11, e0154029. doi: 10.1371/journal.pone.0154029

Espadinha, D., Sobral, R. G., Mendes, C. I., Méric, G., Sheppard, S. K., Carriço, J. A., et al. (2019). Distinct Phenotypic and Genomic Signatures Underlie Contrasting Pathogenic Potential of *Staphylococcus epidermidis* Clonal Lineages. *Front. Microbiol.* 10:1971. doi: 10.3389/fmicb.2019.01971

Feßler, A. T., Zhao, Q., Schoenfelder, S., Kadlec, K., Brenner Michael, G., Wang, Y., et al. (2017). Complete sequence of a plasmid from a bovine methicillin-resistant

Staphylococcus aureus harbouring a novel *ica*-like gene cluster in addition to antimicrobial and heavy metal resistance genes. *Vet. Microbiol.* 200, 95–100. doi: 10.1016/j.vetmic.2016.07.010

Feßler, A., Kadlec, K., Wang, Y., Zhang, W.-J., Wu, C., Shen, J., et al. (2018). Small Antimicrobial Resistance Plasmids in Livestock-Associated Methicillin-Resistant *Staphylococcus aureus* CC398. *Front. Microbiol.* 9:2063. doi: 10.3389/fmicb.2018.02063

Fey, P. D., and Olson, M. E. (2010). Current concepts in biofilm formation of *Staphylococcus epidermidis*. *Future Microbiol.* 5, 917–933. doi: 10.2217/fmb.10.56

Firth, N., Jensen, S. O., Kwong, S. M., Skurray, R. A., and Ramsay, J. P. (2018). Staphylococcal Plasmids, Transposable and Integrative Elements. *Microbiol. Spectr.* 6. doi: 10.1128/microbiolspec.GPP3-0030-2018

Fluckiger, U., Ulrich, M., Steinhuber, A., Döring, G., Mack, D., Landmann, R., et al. (2005). Biofilm formation, *icaADBC* transcription, and polysaccharide intercellular adhesin synthesis by staphylococci in a device-related infection model. *Infect. Immun.* 73, 1811–1819. doi: 10.1128/IAI.73.3.1811-1819.2005

Foster, T. J. (2017). Antibiotic resistance in *Staphylococcus aureus*. Current status and future prospects. *FEMS Microbiol. Rev.* 41, 430–449. doi: 10.1093/femsre/fux007

Geiger, T., Francois, P., Liebeke, M., Fraunholz, M., Goerke, C., Krismer, B., et al. (2012). The stringent response of *Staphylococcus aureus* and its impact on survival after phagocytosis through the induction of intracellular PSMs expression. *PLoS Pathog.* 8, e1003016. doi: 10.1371/journal.ppat.1003016

Gill, S. R., Fouts, D. E., Archer, G. L., Mongodin, E. F., Deboy, R. T., Ravel, J., et al. (2005). Insights on evolution of virulence and resistance from the complete genome analysis of an early methicillin-resistant *Staphylococcus aureus* strain and a biofilm-producing methicillin-resistant *Staphylococcus epidermidis* strain. *J. Bacteriol.* 187, 2426–2438. doi: 10.1128/JB.187.7.2426-2438.2005

Heilmann, C., Schweitzer, O., Gerke, C., Vanittanakom, N., Mack, D., and Götz, F. (1996). Molecular basis of intercellular adhesion in the biofilm-forming *Staphylococcus epidermidis*. *Mol. Microbiol.* 20, 1083–1091. doi: 10.1111/j.1365-2958.1996.tb02548.x

Heilmann, C., Ziebuhr, W., and Becker, K. (2019). Are coagulase-negative staphylococci virulent? *Clin. Microbiol. Infect.* 25, 1071–1080. doi: 10.1016/j.cmi.2018.11.012

Hoang, T.-M., Zhou, C., Lindgren, J. K., Galac, M. R., Corey, B., Endres, J. E., et al. (2019). Transcriptional Regulation of *icaADBC* by both IcaR and TcaR in *Staphylococcus epidermidis*. *J. Bacteriol.* 201, 1–17. doi: 10.1128/jb.00524-18

Huang, M. L., Cangelosi, G. A., Halperin, W., and Nester, E. W. (1990). A chromosomal *Agrobacterium tumefaciens* gene required for effective plant signal transduction. *J. Bacteriol.* 172, 1814–1822. doi: 10.1128/jb.172.4.1814-1822.1990

Jefferson, K. K., Cramton, S. E., Götz, F., and Pier, G. B. (2003). Identification of a 5-nucleotide sequence that controls expression of the *ica* locus in *Staphylococcus aureus* and characterization of the DNA-binding properties of IcaR. *Mol. Microbiol.* 48, 889–899. doi: 10.1046/j.1365-2958.2003.03482.x

Jefferson, K. K., Pier, D. B., Goldmann, D. A., and Pier, G. B. (2004). The teicoplanin-associated locus regulator (TcaR) and the intercellular adhesin locus regulator (IcaR) are transcriptional inhibitors of the *ica* locus in *Staphylococcus aureus*. *J. Bacteriol.* 186, 2449–2456. doi: 10.1128/jb.186.8.2449-2456.2004

Jeng, W. Y., Ko, T. P., Liu, C. I., Guo, R. T., Liu, C. L., Shr, H. L., et al. (2008). Crystal structure of IcaR, a repressor of the TetR family implicated in biofilm formation in *Staphylococcus epidermidis*. *Nucleic Acids Res.* 36, 1567–1577. doi: 10.1093/nar/gkm1176

Kadlec, K., Feßler, A. T., Hauschild, T., and Schwarz, S. (2012). Novel and uncommon antimicrobial resistance genes in livestock-associated methicillin-resistant *Staphylococcus aureus*. *Clin. Microbiol. Infect.* 18, 745–755. doi: 10.1111/j.1469-0691.2012.03842.x

Kozitskaya, S., Olson, M. E., Fey, P. D., Witte, W., Ohlsen, K., and Ziebuhr, W. (2005). Clonal analysis of *Staphylococcus epidermidis* isolates carrying or lacking biofilm-mediating genes by multilocus sequence typing. *J. Clin. Microbiol.* 43, 4751–4757. doi: 10.1128/JCM.43.9.4751-4757.2005

Kropec, A., Maira-Litran, T., Jefferson, K. K., Grout, M., Cramton, S. E., Götz, F., et al. (2005). Poly-N-acetylglucosamine production in *Staphylococcus aureus* is essential for virulence in murine models of systemic infection. *Infect. Immun.* 73, 6868–6876. doi: 10.1128/IAI.73.10.6868-6876.2005

Kwong, S. M., Ramsay, J. P., Jensen, S. O., and Firth, N. (2017). Replication of Staphylococcal Resistance Plasmids. *Front. Microbiol.* 8:2279. doi: 10.3389/fmicb.2017.02279

Lakhundi, S., and Zhang, K. (2018). Methicillin-Resistant *Staphylococcus aureus*: Molecular Characterization, Evolution, and Epidemiology. *Clin. Microbiol. Rev.* 31. doi: 10.1128/CMR.00020-18

Lee, A. S., de Lencastre, H., Garau, J., Kluytmans, J., Malhotra-Kumar, S., Peschel, A., et al. (2018a). Methicillin-resistant *Staphylococcus aureus*. *Nat. Rev. Dis. Primers* 4, 18033. doi: 10.1038/nrdp.2018.33

Lee, J. Y. H., Monk, I. R., Gonçalves da Silva, A., Seemann, T., Chua, K. Y. L., Kearns, A., et al. (2018b). Global spread of three multidrug-resistant lineages of *Staphylococcus epidermidis*. *Nat. Microbiol.* 3, 1175–1185. doi: 10.1038/s41564-018-0230-7

Lerch, M. F., Schoenfelder, S. M. K., Marincola, G., Wencker, F. D. R., Eckart, M., Förstner, K. U., et al. (2019). A non-coding RNA from the intercellular adhesion (*ica*) locus of *Staphylococcus epidermidis* controls polysaccharide intercellular adhesion (PIA)-mediated biofilm formation. *Mol. Microbiol.* 111, 1571–1591. doi: 10.1111/mmi.14238

Lindgren, J. K., Thomas, V. C., Olson, M. E., Chaudhari, S. S., Nuxoll, A. S., Schaeffer, C. R., et al. (2014). Arginine deiminase in *Staphylococcus epidermidis* functions to augment biofilm maturation through pH homeostasis. *J. Bacteriol.* 196, 2277–2289. doi: 10.1128/JB.00051-14

Mack, D., Fischer, W., Krokotsch, A., Leopold, K., Hartmann, R., Egge, H., et al. (1996). The intercellular adhesin involved in biofilm accumulation of *Staphylococcus epidermidis* is a linear beta-1,6-linked glucosaminoglycan: purification and structural analysis. *J. Bacteriol.* 178, 175–183. doi: 10.1128/jb.178.1.175-183.1996

Madeira, F., Park, Y., Lee, J., Buso, N., Gur, T., Madhusoodanan, N., et al. (2019). The EMBL-EBI search and sequence analysis tools APIs in 2019. *Nucleic Acids Res.* 47, W636–W641. doi: 10.1093/nar/gkz268

Madhaiyan, M., Wirth, J. S., and Saravanan, V. S. (2020). Phylogenomic analyses of the Staphylococcaceae family suggest the reclassification of five species within the genus *Staphylococcus* as heterotypic synonyms, the promotion of five subspecies to novel species, the taxonomic reassignment of five *Staphylococcus* species to *Mammaliicoccus* gen. nov., and the formal assignment of *Nosocomiicoccus* to the family Staphylococcaceae. *Int. J. Syst. Evol. Microbiol.* 70, 5926–5936. doi: 10.1099/ijsem.0.004498

Marincola, G., Wencker, F. D. R., and Ziebuhr, W. (2019). The Many Facets of the Small Non-coding RNA RsaE (RoxS) in Metabolic Niche Adaptation of Gram-Positive Bacteria. *J. Mol. Biol.* 431, 4684–4698. doi: 10.1016/j.jmb.2019.03.016

Méric, G., Miragaia, M., de Been, M., Yahara, K., Pascoe, B., Mageiros, L., et al. (2015). Ecological Overlap and Horizontal Gene Transfer in *Staphylococcus aureus* and *Staphylococcus epidermidis*. *Genome Biol. Evol.* 7, 1313–1328. doi: 10.1093/gbe/evv066

Méric, G., Mageiros, L., Pensar, J., Laabei, M., Yahara, K., Pascoe, B., et al. (2018). Disease-associated genotypes of the commensal skin bacterium *Staphylococcus epidermidis*. *Nat. Commun.* 9, 5034. doi: 10.1038/s41467-018-07368-7

Monk, I. R., Shah, I. M., Xu, M., Tan, M.-W., and Foster, T. J. (2012). Transforming the untransformable: application of direct transformation to manipulate genetically *Staphylococcus aureus* and *Staphylococcus epidermidis*. *MBio* 3. doi: 10.1128/mBio.00277-11

Nair, D., Memmi, G., Hernandez, D., Bard, J., Beaume, M., Gill, S., et al. (2011). Whole-genome sequencing of *Staphylococcus aureus* strain RN4220, a key laboratory strain used in virulence research, identifies mutations that affect not only virulence factors but also the fitness of the strain. *J. Bacteriol.* 193, 2332–2335. doi: 10.1128/JB.00027-11

Nguyen, H. T. T., Nguyen, T. H., and Otto, M. (2020). The staphylococcal exopolysaccharide PIA - Biosynthesis and role in biofilm formation, colonization, and infection. *Comput. Struct. Biotechnol. J.* 18, 3324–3334. doi: 10.1016/j.csbj.2020.10.027

Nozaki, S., and Niki, H. (2019). Exonuclease III (XthA) Enforces *In Vivo* DNA Cloning of *Escherichia coli* To Create Cohesive Ends. *J. Bacteriol.* 201, 1–13. doi: 10.1128/JB.00660-18

Qin, Z., Ou, Y., Yang, L., Zhu, Y., Tolker-Nielsen, T., Molin, S., et al. (2007). Role of autolysin-mediated DNA release in biofilm formation of *Staphylococcus epidermidis*. *Microbiology* 153, 2083–2092. doi: 10.1099/mic.0.2007/006031-0

Que, Y.-A., Haefliger, J.-A., Piroth, L., François, P., Widmer, E., Entenza, J. M., et al. (2005). Fibrinogen and fibronectin binding cooperate for valve infection and invasion in *Staphylococcus aureus* experimental endocarditis. *J. Exp. Med.* 201, 1627–1635. doi: 10.1084/jem.20050125

Rochat, T., Bohn, C., Morvan, C., Le Lam, T. N., Razvi, F., Pain, A., et al. (2018). The conserved regulatory RNA RsaE down-regulates the arginine degradation pathway in *Staphylococcus aureus*. *Nucleic Acids Res.* 46, 8803–8816. doi: 10.1093/nar/gky584

Rohde, H., Burdelski, C., Bartscht, K., Hussain, M., Buck, F., Horstkotte, M. A., et al. (2005). Induction of *Staphylococcus epidermidis* biofilm formation via proteolytic processing of the accumulation-associated protein by staphylococcal and host proteases. *Mol. Microbiol.* 55, 1883–1895. doi: 10.1111/j.1365-2958.2005.04515.x

Ruiz de los Mozos, I., Vergara-Irigaray, M., Segura, V., Villanueva, M., Bitarte, N., Saramago, M., et al. (2013). Base pairing interaction between 5'- and 3'-UTRs controls *icaR* mRNA translation in *Staphylococcus aureus*. *PLoS Genet.* 9, e1004001. doi: 10.1371/journal.pgen.1004001

Sadykov, M. R., Hartmann, T., Mattes, T. A., Hiatt, M., Jann, N. J., Zhu, Y., et al. (2011). CcpA coordinates central metabolism and biofilm formation in *Staphylococcus epidermidis*. *Microbiology* 157, 3458–3468. doi: 10.1099/mic.0.051243-0

San Millan, A., and MacLean, R. C. (2017). Fitness Costs of Plasmids: a Limit to Plasmid Transmission. *Microbiol. Spectr.* 5. doi: 10.1128/microbiolspec.MTBP-0016-2017

Schilcher, K., and Horswill, A. R. (2020). Staphylococcal Biofilm Development: Structure, Regulation, and Treatment Strategies. *Microbiol. Mol. Biol. Rev.* 84. doi: 10.1128/MMBR.00026-19

Schoenfelder, S. M. K., Lange, C., Prakash, S. A., Marincola, G., Lerch, M. F., Wencker, F. D. R., et al. (2019). The small non-coding RNA RsaE influences extracellular matrix composition in *Staphylococcus epidermidis* biofilm communities. *PLoS Pathog.* 15, e1007618. doi: 10.1371/journal.ppat.1007618

Schwartbeck, B., Birtel, J., Treffon, J., Langhanki, L., Mellmann, A., Kale, D., et al. (2016). Dynamic *in vivo* mutations within the *ica* operon during persistence of *Staphylococcus aureus* in the airways of cystic fibrosis patients. *PLoS Pathog.* 12, e1006024. doi: 10.1371/journal.ppat.1006024

Seidl, K., Goerke, C., Wolz, C., Mack, D., Berger-Bächi, B., and Bischoff, M. (2008). *Staphylococcus aureus* CcpA affects biofilm formation. *Infect. Immun.* 76, 2044–2050. doi: 10.1128/IAI.00035-08

Slater, F. R., Bailey, M. J., Tett, A. J., and Turner, S. L. (2008). Progress towards understanding the fate of plasmids in bacterial communities. *FEMS Microbiol. Ecol.* 66, 3–13. doi: 10.1111/j.1574-6941.2008.00505.x

Thomas, J. C., Zhang, L., and Robinson, D. A. (2014). Differing lifestyles of *Staphylococcus epidermidis* as revealed through Bayesian clustering of multilocus sequence types. *Infect. Genet. Evol.* 22, 257–264. doi: 10.1016/j.meegid.2013.06.020

Tong, S. Y. C., Davis, J. S., Eichenberger, E., Holland, T. L., and Fowler, V. G. (2015). *Staphylococcus aureus* infections: epidemiology, pathophysiology, clinical manifestations, and management. *Clin. Microbiol. Rev.* 28, 603–661. doi: 10.1128/CMR.00134-14

Venanzio, G., Moon, K. H., Weber, B. S., Lopez, J., Ly, P. M., Potter, R. F., et al. (2019). Multidrug-resistant plasmids repress chromosomally encoded T6SS to enable their dissemination. *Proc. Natl. Acad. Sci. U. S. A.* 116, 1378–1383. doi: 10.1073/pnas.1812557116

Vial, L., and Hommais, F. (2020). Plasmid-chromosome cross-talks. *Environ. Microbiol.* 22, 540–556. doi: 10.1111/1462-2920.14880

Vuong, C., Kidder, J. B., Jacobson, E. R., Otto, M., Proctor, R. A., and Somerville, G. A. (2005). *Staphylococcus epidermidis* polysaccharide intercellular adhesin production significantly increases during tricarboxylic acid cycle stress. *J. Bacteriol.* 187, 2967–2973. doi: 10.1128/JB.187.9.2967-2973.2005

Wang, X., Preston, J. F., and Romeo, T. (2004). The *pgaABCD* locus of *Escherichia coli* promotes the synthesis of a polysaccharide adhesin required for biofilm formation. *J. Bacteriol.* 186, 2724–2734. doi: 10.1128/jb.186.9.2724-2734.2004

Waterhouse, A. M., Procter, J. B., Martin, D. M. A., Clamp, M., and Barton, G. J. (2009). Jalview Version 2–a multiple sequence alignment editor and analysis workbench. *Bioinformatics* 25, 1189–1191. doi: 10.1093/bioinformatics/btp033

Zhu, Y., Xiong, Y. Q., Sadykov, M. R., Fey, P. D., Lei, M. G., Lee, C. Y., et al. (2009). Tricarboxylic acid cycle-dependent attenuation of *Staphylococcus aureus in vivo* virulence by selective inhibition of amino acid transport. *Infect. Immun.* 77, 4256–4264. doi: 10.1128/IAI.00195-09